Front. Environ. Sci. Eng. 2023, 17(9): 106
https://doi.org/10.1007/s11783-023-1706-0

RESEARCH ARTICLE

Insights into the electron transfer mechanisms of permanganate activation by carbon nanotube membrane for enhanced micropollutants degradation

Xufang Wang[1], Dongli Guo[1], Jinna Zhang[2], Yuan Yao (✉)[3], Yanbiao Liu (✉)[1,4]

1 College of Environmental Science and Engineering, Donghua University, Shanghai 201620, China
2 State Key Laboratory of Urban Water Resource and Environment, School of Environment, Harbin Institute of Technology, Harbin 150090, China
3 MIIT Key Laboratory of Critical Materials Technology for New Energy Conversion and Storage, School of Chemistry and Chemical Engineering, Harbin Institute of Technology, Harbin 150080, China
4 Shanghai Institute of Pollution Control and Ecological Security, Shanghai 200092, China

HIGHLIGHTS

- A CNT filter enabled effective $KMnO_4$ activation via facilitated electron transfer.
- Ultra-fast degradation of micropollutants were achieved in $KMnO_4$/CNT system.
- CNT mediated electron transfer process from electron-rich molecules to $KMnO_4$.
- Electron transfer dominated organic degradation.

ARTICLE INFO

Article history:
Received 1 February 2023
Revised 18 February 2023
Accepted 22 February 2023
Available online 1 April 2023

Keywords:
$KMnO_4$
Carbon nanotubes
Non-radical pathway
Electron transfer
Water treatment

GRAPHIC ABSTRACT

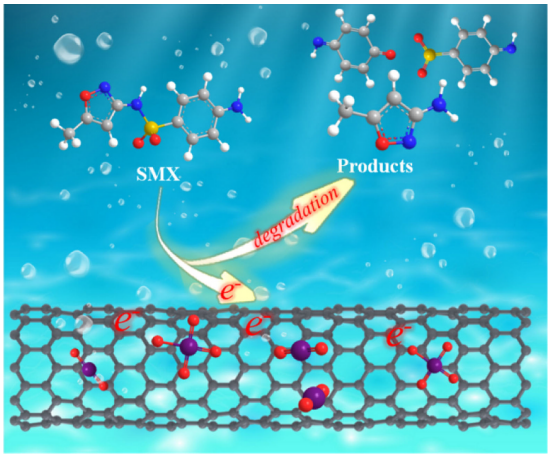

ABSTRACT

Numerous reagents have been proposed as electron sacrificers to induce the decomposition of permanganate ($KMnO_4$) by producing highly reactive Mn species for micropollutants degradation. However, this strategy can lead to low $KMnO_4$ utilization efficiency due to limitations associated with poor mass transport and high energy consumption. In the present study, we rationally designed a catalytic carbon nanotube (CNT) membrane for $KMnO_4$ activation toward enhanced degradation of micropollutants. The proposed flow-through system outperformed conventional batch reactor owing to the improved mass transfer via convection. Under optimal conditionals, a > 70% removal (equivalent to an oxidation flux of 2.43 mmol/(h·m^2)) of 80 μmol/L sulfamethoxazole (SMX) solution can be achieved at single-pass mode. The experimental analysis and DFT studies verified that CNT could mediate direct electron transfer from organic molecules to $KMnO_4$, resulting in a high utilization efficiency of $KMnO_4$. Furthermore, the $KMnO_4$/CNT system had outstanding reusability and CNT could maintain a long-lasting reactivity, which served as a green strategy for the remediation of micropollutants in a sustainable manner. This study provides new insights into the electron transfer mechanisms and unveils the advantages of effective $KMnO_4$ utilization in the $KMnO_4$/CNT system for environmental remediation.

✉ Corresponding authors
E-mails: yanbiaoliu@dhu.edu.cn (Y. Liu); yyuan@hit.edu.cn (Y. Yao)

1 Introduction

With the rapid growth of industrialization, toxic and non-biodegradable organic micropollutants of industrial origin are discharged into the environment directly or indirectly with a rise in environmental concerns regarding water pollution (Liu et al., 2009; Liu et al., 2018; Rasool et al., 2019). Different water treatment approaches, such as flocculation, bio-degradation, and physical adsorption, are not effective in dealing with organic contaminants (OCs) because of their chemical persistence, high toxicity and low concentration (Liu et al., 2009; Zheng et al., 2021; Shen et al., 2022). To meet the requirement of environmental remediation, advanced oxidation process has emerged as a viable technology for the abatement of different recalcitrant OCs in water due to their environmental friendliness and high efficiency (Zhou et al., 2019; Mustafa et al., 2021).

As a potential chemical oxidant, permanganate ($KMnO_4$) has been widely studied for water decontamination due to its high efficiency, cost-effectiveness and high stability (Guan et al., 2010; Ma et al., 2011; Chen et al., 2016; Shi et al., 2020). However, the poor stability and limited oxidation potential (1.68 V) of $KMnO_4$ restrict its applications in several circumstances (Bavasso et al., 2020). Hence, various innovative approaches have been attempted to boost the reactivity of $KMnO_4$ by producing highly reactive intermediate manganese species, such as ligands (Jiang et al., 2010), bisulfite (Cheng et al., 2019), electricity (Zhu et al., 2019a), ultraviolet irradiation (Hu et al., 2018). However, because of the addition of toxic and expensive chemicals and the occurrence of secondary pollution, these routes strongly impede the scientific progress of $KMnO_4$ oxidation toward practical applications.

In recent years, metal-free carbon material has emerged as an attractive additive to $KMnO_4$ oxidation due to its environmental friendliness. For instance, biochar was used as an electron sacrificer to enhance $KMnO_4$ oxidation by producing reactive manganese species (Tian et al., 2019). However, the reactivity of biochar is temporary due to the unattainable regeneration of reductive sites (Derakhshani and Naghizadeh, 2013). Moreover, the quenching effects of varying species strongly decreased the utilization efficiency of $KMnO_4$. Alternatively, carbon nanotubes (CNT), an excellent electron transfer mediator, had been proved as a 'bridge' to facilitate the electron delivery from organic molecules (electron donor) to persulfate (electron acceptors) (Han et al., 2019; Hao et al., 2019; Shao et al., 2020). This may lead to oxidative decomposition of OCs, rather than converting from $KMnO_4$ to reactive manganese species (Peng et al., 2021; Wang et al., 2021).

With regard to mass transport limitation, conventional chemical oxidation methods mainly employ batch-mixed mode, and the mass transport between the reactants and catalyst surface is often diffusion-limited. Alternatively, a flow-through system may serve as a crucial strategy to avoid this limitation *via* convection-regulated mass transport. Compared with conventional batch system, there are quantitative enhancements in the overall reaction kinetics realized by the flow-through system (Liu et al., 2020). Importantly, these one-dimensional CNT can be readily assembled into three-dimensional and porous networks, allowing for flow-through operation.

Herein, we design and establish a flow-through $KMnO_4$/CNT system, where CNT was chosen as an electron mediator to simultaneously improve the oxidation ability and utilization efficiency of $KMnO_4$. Sulfamethoxazole (SMX) was selected as the target compound due to its chemical persistence and ubiquitous distribution. The effects of several operational parameters were determined and optimized. The reaction mechanism was systematically explored according to a combination of experimental data and density functional theory (DFT) calculations by identifying reactive Mn species and analyzing the direct electron transfer from organic molecules to $KMnO_4$. Besides, we comparatively investigated the utilization efficiency of $KMnO_4$ in different systems. Furthermore, ultraperformance liquid chromatography−quadrupole time-of-flight premier mass spectrometry (UPLC-QTOF-MS/MS) was used to unveil the SMX degradation pathway. Toxicity estimation software was employed to assess the toxicity of the intermediates based on quantitative structure–activity relationship (QSAR) prediction. Overall, this study reveals that CNT mediates electron transfer from SMX to $KMnO_4$ and presents the rational design of a robust, effective, and viable flow-through $KMnO_4$/CNT system toward green environmental remediation.

2 Materials and methods

2.1 Reagents and chemicals

Details on the reagents and chemicals used in thus study are summarized in Text S1. All chemical reagents were employed without further purification. Ultrapure water (resistivity $\geqslant$ 18.2 MΩ·cm) was utilized throughout the experiments.

2.2 Equipment and experimental procedures

The filtration trials were performed in a commercial Whatman polycarbonate filtration casing at ambient temperature (25 ± 1°C). Details on the fabrication of CNT filters were available in Text S2. To eliminate any contributions from physical adsorption, all experiments were carried out after achieving filter adsorption satura-

tion by flowing through 80 μmol/L of SMX solution for 3 h at 0.5 mL/min, as controlled by an Ismatec ISM833C peristaltic pump (Switzerland). In a typical experiment, freshly prepared SMX solution with certain amount of $KMnO_4$ was passed through the filtration system at a flow rate of 0.5 mL/min in a single-pass filtration mode. Solution pH was adjusted using 1.0 mmol/L HCl and/or NaOH. At pre-determined time intervals, 1.0 mL samples were collected. The liquid samples were immediately filtered through a polytetrafluoroethylene membrane (PTFE, 0.22 μm) and mixed with 50 μL hydroxylamine hydrochloride (1.0 mol/L) to terminate any radical reactions. Oxidation flux was used to quantify the filtration performance, and the calculation equation was described in Text S3. All experiments were repeated in triplicate to ensure reproducibility.

2.3 Characterization

The crystal phase of pristine CNT filter specimens was determined by X-ray diffractometer (XRD, Rigaku D/max-2550PC, λ = 1.5406 Å). X-ray photoelectron spectroscopy (XPS, ESCALAB 250Xi, Thermo Fisher Scientific Escalab 250Xi) was applied to examine the variation on the chemical states on the CNT surface. Any generated reactive oxygen species (ROS) were identified using an EMXnano spectrometer (Bruker, Germany) with 5,5-dimethyl-1-pyrrolidine-N-oxide (DMPO) or 2,2,6,6-tetramethylpiperidine (TEMP). Chronoamperometry was conducted in 50 mmol/L Na_2SO_4 solution using a CHI 660E electrochemical workstation in a typical three-electrode system (e.g., a CNT working electrode, a saturated Ag/AgCl reference electrode and a Ti sheet counter electrode).

2.4 Analytical methods and calculations

High-performance liquid chromatography (HPLC, Shimadzu LC-16) coupled to a ShimNex UP C18 column (5 μm, 4.6 mm × 150 mm) was applied to determine the concentration of micropollutants. Details on the analytical protocols and operational parameters were summarized in Table S1. The concentration of $KMnO_4$ was determined using a UV2600 spectrophotometer (Shimadzu) at 525 nm. Sodium pyrophosphate (PP) was applied to determine the content of $Mn(III)_{aq}$ by forming a stabilized complex with $Mn(III)_{aq}$ (i.e., PP-Mn(III)) characterized by a 258-nm absorbance peak (Sun et al., 2015). The characteristic absorption peaks of Mn(VI) and Mn(V) were centered at 610 and 660 nm, respectively (Simandi et al., 1984). The SMX intermediates were quantified by a liquid chromatography-mass spectrometry (LC-MS, Agilent LC1290-QQQ-6470). Theoretical calculations of SMX degradation according to the density functional theory (DFT) were conducted via Gaussian 16 suite of programs. Details are available in Text S4. The quantitative structure activity relationship (QSAR) method was executed to analyze the mutagenicity, bioaccumulation factor, acute toxicity and developmental toxicity of SMX and its intermediates *via* Toxicity Estimation Software Tool (T.E.S.T., US, EPA). Details were available in Text S5.

3 Results and discussion

3.1 Ultrafast water decontamination by $KMnO_4$/CNT system

The catalytic performance of $KMnO_4$/CNT flow-through system was indirectly assessed by organic oxidative flux. To investigate the catalytic activity of CNT filter toward $KMnO_4$, SMX was chosen as a model sulfonamide antibiotic. $KMnO_4$, as a strong oxidizing agent, may be able to oxidize SMX directly. The results revealed a moderate SMX oxidation ability at an elevated concentration of $KMnO_4$ in the $KMnO_4$-alone system (Fig. 1(a)). For example, negligible SMX was removed at a $KMnO_4$

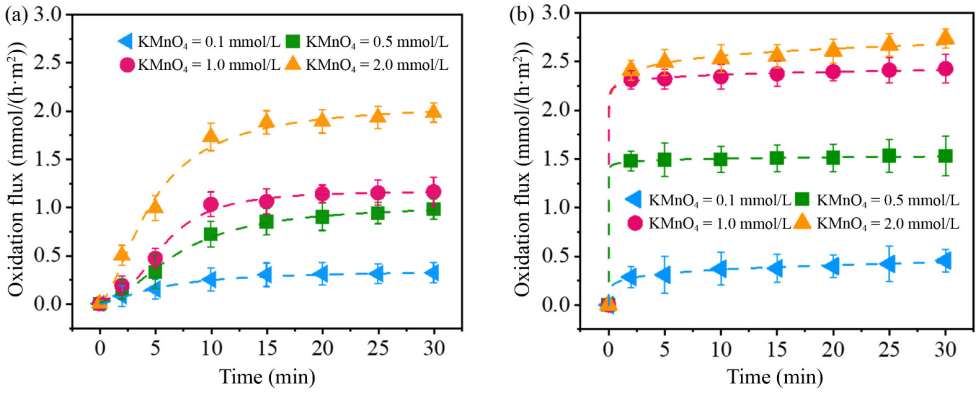

Fig. 1 SMX oxidation flux under different $KMnO_4$ concentrations in the (a) $KMnO_4$ alone system and (b) CNT/$KMnO_4$ system. Experimental conditions: $[SMX]_0$ = 80 μmol/L, flow rate = 0.5 mL/min, and pH = 6.2.

concentration of 0.1 mmol/L, while a 1.98 mmol/(h·m^2) SMX oxidation flux was observed at a $KMnO_4$ concentration of 2.0 mmol/L. As displayed in Fig. 1(b), the SMX oxidation flux increased from 0.46 to 2.43 mmol/(h·m^2) with the $KMnO_4$ concentration increasing from 0.1 to 1.0 mmol/L in the $KMnO_4$/CNT system. This may be attributed to an increased number of electron acceptors with increasing $KMnO_4$ concentrations, and thus, more electrons are transferred from SMX to $KMnO_4$ with the mediation of CNT (Peng et al., 2021). It is worth noting that the SMX oxidation flux only increased from 2.43 to 2.74 mmol/(h·m^2) when $KMnO_4$ concentration further increased from 1.0 to 2.0 mmol/L, which might due to the limitation of CNT dosage, i.e., the dosage of CNT limited the electron transport capacity of the system (Peng et al., 2021). To be specific, the SMX oxidation flux was 2.43 mmol/(h·m^2) in the $KMnO_4$/CNT system, which was significantly higher compared to the $KMnO_4$ alone system (1.16 mmol/(h·m^2)) at a $KMnO_4$ concentration of 1.0 mmol/L. More importantly, the SMX oxidation can be profoundly improved by coupling with CNT, demonstrating the excellent reactivity of CNT toward the activation of $KMnO_4$.

3.2 Mechanistic investigation

The underlying mechanism of $KMnO_4$/CNT was explored by identifying the reactive species and exploring the potential role of electron transfer pathway.

3.2.1 Permanganate consumption in different processes

As shown in Fig. S1, 100 μmol/L $KMnO_4$ could be directly consumed by raw CNT in the absence of SMX. Although raw CNT possess a low electron-donating ability, it can give up electrons toward the $KMnO_4$ degradation (Zhang et al., 2022). This indicates that $KMnO_4$ may interact with CNT, but the reaction rate is rather slow. Besides, the utilization of $KMnO_4$ with SMX was evidently greatly than that without SMX. For example, only 30 μmol/L $KMnO_4$ without SMX was utilized in the $KMnO_4$/CNT system, whereas the utilization of $KMnO_4$ with 80 μmol/L SMX increased sharply to 340 μmol/L. These results further demonstrate that the reaction of $KMnO_4$ with CNT is sluggish and after addition of SMX into the $KMnO_4$/CNT system, the oxidation ability of $KMnO_4$ is significantly promoted. $KMnO_4$ degradation is largely dependent on the electron-donating effect of SMX *via* an electron-transfer pathway, which is contradictory to that of $KMnO_4$ activation by electron sacrificers. Hence, the interaction of $KMnO_4$ with electron donors may reduce the utilization efficiency of $KMnO_4$. Alternatively, direct electron-transfer mechanisms of the $KMnO_4$/CNT system could avoid $KMnO_4$ degradation, leading to an increase in $KMnO_4$ utilization efficiency.

3.2.2 Evaluating the contribution of diverse reactive species in the $KMnO_4$/CNT system

In the $KMnO_4$-based system, certain intermediates, such as manganese divalent ion ($Mn(II)_{aq}$), trivalent manganese ($Mn(III)_{aq}$), manganite ($Mn(VI)_{aq}$), hypomanganate ($Mn(V)_{aq}$) and manganese oxide ($Mn(IV)_s$), could be produced. Therefore, reactive Mn species (e.g., Mn(III), Mn(IV), Mn(V) and Mn(VI)) are often considered as the primary oxidative species for the degradation of contaminants (Chen et al., 2020). High-valence Mn species, such as Mn(V) and Mn(VI), may be formed and promotes the oxidation of contaminants during the $KMnO_4$ consumption (Gao et al., 2019). Methyl phenyl sulfoxide (PMSO) was chosen as scavengers for high metal-oxo species (e.g. Mn(V) and Mn(VI)) (Chen et al., 2020). Results suggested that the transformation kinetics of PMSO to $PMSO_2$ was similar regardless of the presence of CNT or not (Fig. S2). This indicated that a negligible contribution on the SMX degradation from high-valent Mn species (i.e., Mn(VI) and Mn(V)) in the $KMnO_4$/CNT system. Meanwhile, as shown in Fig. 2(a), the spike of PMSO cannot influence the SMX oxidation flux in the $KMnO_4$/CNT system. Besides, no characteristic peaks associated with Mn(V) and Mn(VI) were identified (Fig. 2(b)). Thus, excluding the formation and contribution of Mn(V) and Mn(VI) in this system (Chen et al., 2020).

Previous literature reported that MnO_2 with a moderate redox potential (E_h = 0.464 V) could directly oxidize OCs or promote the removal of OCs via oxidation and adsorption (Gao et al., 2012; Sun et al., 2019; Pan et al., 2021; Wang et al., 2021). To analyze these Mn intermediates on CNT surface, the surface characteristics of CNT pre- and post-reaction were assessed by XPS technique. As shown in Fig. 3(a), compared to the raw CNT, Mn elemental peak was determined on the surface of used CNT. In parallel, as shown in Fig. 3(b), Mn 2p3/2 photoelectron spectrum of used CNT was observed at the binding energy 642.0 eV and 643.8 eV, which can be assigned to Mn(IV). Additionally, the high-resolution O 1s spectrum of the raw CNT (Fig. 3(c)) located at 532.2 eV can be assigned to the surface of hydroxyl species (Yang et al., 2019). Compared with the raw CNT, a new peak (at 529.9 eV) appeared in the O 1s core level for the used CNT, which belonged to adsorbed Mn-O bonds on the CNT surface (Du et al., 2020). The results revealed that MnO_2 was formed and adsorbed on CNT surface during the reaction. To analyze the reactivity of Mn(IV), *ex situ* synthesized MnO_2 colloid was added dropwise into the $KMnO_4$/CNT system to assess the effects of MnO_2 on the SMX oxidation kinetics. Of note, this *ex situ* spiked MnO_2 colloid was according to the maximum consumption of $KMnO_4$ in the $KMnO_4$/CNT system (340 μmol/L, Fig. S1). As displayed in Fig. 2(c), the MnO_2/CNT system only showed a slight SMX oxidation flux of 0.42 mmol/(h·m^2). Besides, no evident differences in

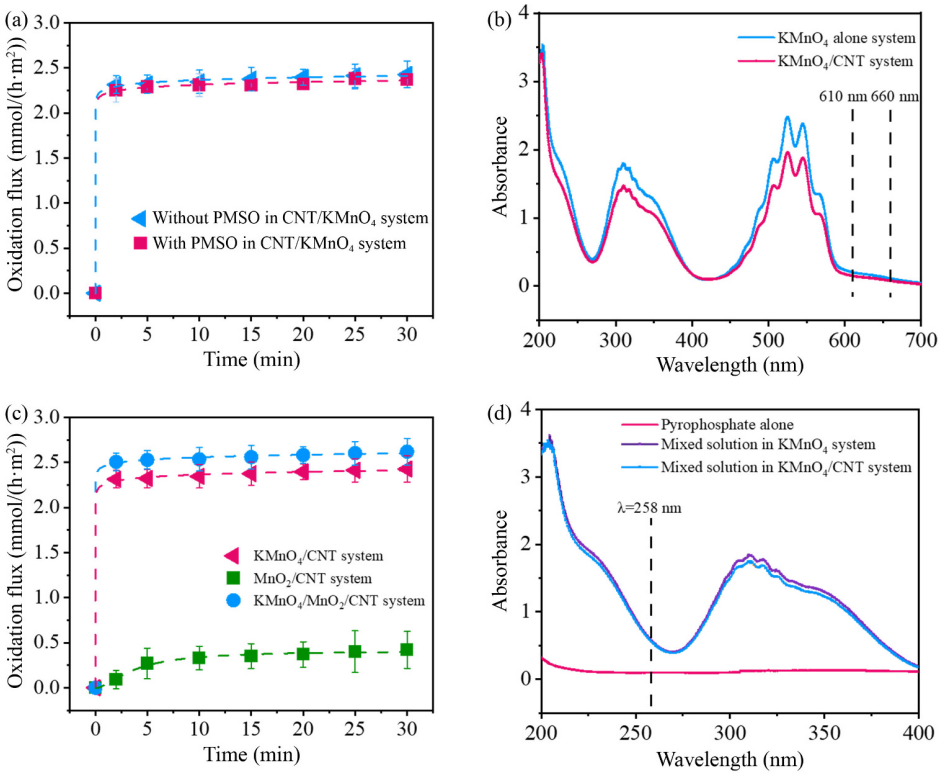

Fig. 2 (a) The effect of PMSO on SMX oxidation in the CNT/$KMnO_4$ system, (b) UV-visible spectrum of different solution samples, (c) SMX oxidation in various systems, (d) UV-visible spectrum of different solution samples in the presence of 1.0 mmol/L pyrophosphate. Experimental conditions: $[SMX]_0$ = 80 μmol/L, $[KMnO_4]_0$ = 1.0 mmol/L, flow rate = 0.5 mL/min, and pH = 6.2.

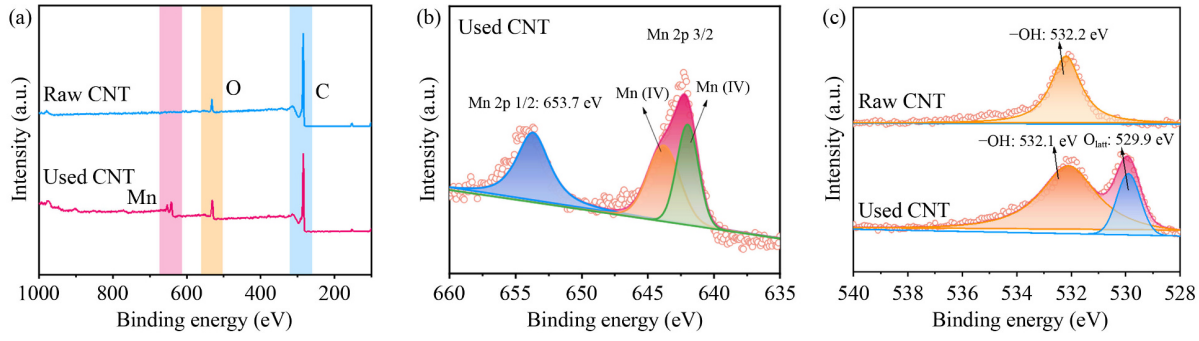

Fig. 3 XPS spectra of CNT: (a) survey spectrum, core-level spectra of (b) Mn 2p and (c) O 1s.

terms of SMX oxidation was observed between the $KMnO_4$/CNT and $KMnO_4/MnO_2$/CNT system (Fig. 2(c), 2.42 mmol/(h·m^2) *vs.* 2.62 mmol/(h·m^2), respectively), suggesting that the contribution from the *in situ* formed MnO_2 on SMX oxidation is rather limited.

It has been reported that Mn(III) obtained from $KMnO_4$ possess moderate oxidative ability (E_h = 1.51 V) toward OCs (Kostka et al., 1995; Zhu et al., 2019b). Therefore, to identify whether Mn(III) was involved in the system, the colorimetric determination of Mn(III)-pyrophosphate complex at a wavelength of 258 nm was detected (Zhu et al., 2019a; Zhu et al., 2019b). However, as displayed in Fig. 2(d), no obvious peak associated with Mn(III)-pyrophosphate complex was emerged. Thus, this excluded the possibility of Mn(III) production and its role in SMX decomposition.

Electron paramagnetic resonance spectrometer (EPR) analysis was conducted with the spin trapping agents TEMP and DMPO targeting $^1O_2$ and $HO^{\cdot}$, respectively. As displayed in Figs. S3a and S3b, the characteristic adduct signals were undetectable, thus excluding the possibility of ROS production in the $KMnO_4$/CNT system. The above discussion collectively indicated that the limited contribution from reactive Mn and oxygen species toward the degradation of SMX. Therefore, we hypothesize that other reactive mechanism may be

involved in SMX degradation in the $KMnO_4$/CNT system.

3.2.3 CNT mediates electron transfer from SMX to permanganate

In recent years, numerous researchers demonstrated that nanoscale carbon materials could mediate electron transfer from OCs to persulfate is the main pathway for OCs oxidation in persulfate-based oxidation systems (Ren et al., 2020; Zhou et al., 2021; Guo et al., 2022; Wu et al., 2022; Yu et al., 2023). Electrochemical characterization was an excellent technique to analyze the electrochemical characteristics of the electrode materials. For example, chronoamperometry tests had been employed to monitor the electron transfer process from the OCs to persulfate, and current density markedly elevated in the co-presence of persulfate and organic substrate on the carbon electrodes (Lee et al., 2016; Tang et al., 2018; Zhu et al., 2018; Jin et al., 2022). As a typical carbon-based material, CNT can also regulate the electron shuttle from SMX to $KMnO_4$ in the $KMnO_4$/CNT system. As displayed in Fig. 4(a), chronoamperometry was further performed to record the charge migration between $KMnO_4$ and SMX. When $KMnO_4$ was added into the system, the occurrence of a negative current showed the rapid electron transfer from CNT to $KMnO_4$. Afterward, the current intensities were further strengthened with the addition of SMX. Hence, the adsorption/electron transfer represents the most likely mechanism of action, i.e., the SMX was first adsorbed by CNT, and then directly electron transfer to $KMnO_4$ with CNT employed as an electron channel (Fig. 4(b)). These results indicated the critical role of the electron transfer-mediated nonradical oxidation pathway in the $KMnO_4$/CNT system. Under the CNT mediation, $KMnO_4$ could directly oxidize the OCs via the electron transfer pathway, and ultimately transform into MnO_2.

$$\mathrm{SMX} + \mathrm{KMnO_4} \xrightarrow{\mathrm{CNT}} \mathrm{intermediates} + \mathrm{MnO_2} \quad (1)$$

To further confirm this hypothesis, DFT calculations were conducted to evaluate the highest occupied molecular orbital (HOMO)-least unoccupied molecular orbital (LUMO) gaps of CNT, SMX, and permanganate. In general, HOMO indicates that electrons are more likely to escape, which can be easily attacked (Pearson, 1986; Casida et al., 1998). As shown in Table S2 and Fig. 5, the HOMO of SMX (−6.108563 eV) was more negative than the LUMO of CNT (−3.008827 eV), suggesting that the electrons of SMX could migrate from SMX to CNT (Han et al., 2019; Shao et al., 2020). Moreover, the electrons transported from the LUMO to HOMO of CNT because of the least energy gap (0.523347 eV) (Yun et al., 2018; Chen et al., 2020). Furthermore, the electrons transferred from the HOMO of CNT (−3.532174 eV) to the LUMO of permanganate (−2.585211 eV) for the decomposition of permanganate (Shao et al., 2020). DFT calculations indicated that CNT-mediated electron transfer from SMX to $KMnO_4$ was influenced by energy gaps. By integrating the above electrochemical analysis and theoretical data, we concluded that CNT could function as an electron mediator to accelerate electron transfer from SMX to $KMnO_4$, thus leading to SMX oxidation and $KMnO_4$ decomposition.

3.3 Proposed SMX degradation pathways and toxicity assessment of the intermediates

The intermediates formed during SMX decomposition were identified using the HPLC-MS technique (Table S3 and Fig. S4). Three plausible SMX decomposition pathways are proposed according to the product identification. As shown in Fig. S5, in pathway I, the C–S bond can be hydrolyzed in the reaction process, leading to the formation of TP1 (m/z = 110.0606) and TP2 (m/z = 99.0558). In pathway II, N11 of SMX can also be oxidized to form TP3 (m/z = 284.0348), which is the classical oxidation product of SMX. Next, TP4 (m/z = 300.0296) can be formed by TP3 transformation. In pathway III, TP5 (m/z = 503.0816) may be a self-

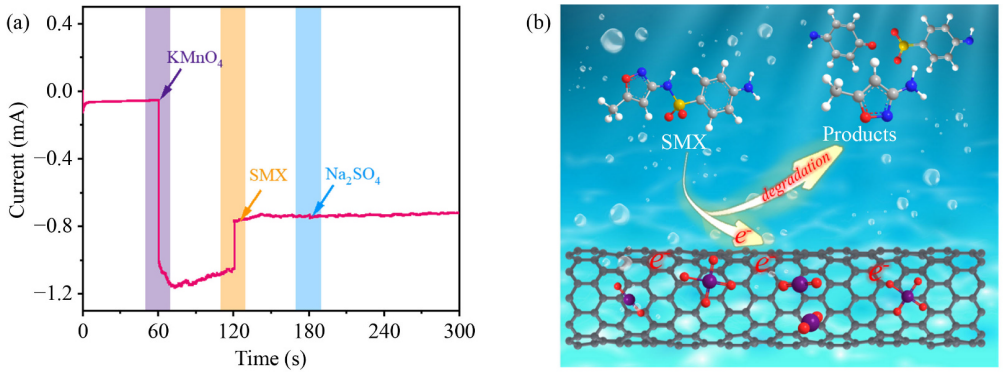

Fig. 4 (a) Chronoamperometry in 50 mmol/L Na_2SO_4 electrolyte solution at Pt electrodes and (b) proposed mechanisms of SMX oxidation in the CNT/$KMnO_4$ system.

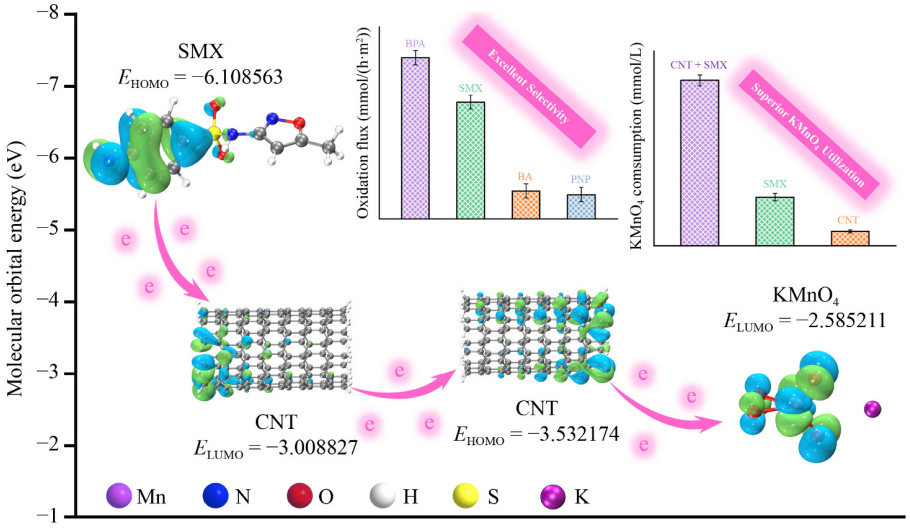

Fig. 5 The potential difference in molecular orbitals drives electron transmission via the structural defects of CNT.

coupling product formed by the coupling reaction of amino groups of two SMX molecules due to N11 of SMX. Finally, the above intermediates can be further transformed into small-molecule products, including TP2 (*m/z* = 99.0558), TP6 (*m/z* = 155.003) and TP7 (*m/z* = 108.0451)

The toxicity estimation of SMX intermediates is also a manifestation of the application potential of the CNT/$KMnO_4$ system. As displayed in Fig. S6a, all the intermediates have negative mutagenicity, including SMX. In addition, for oral rat LD_{50} and bioaccumulation factor, all the intermediates have lower toxicity than SMX (Figs. S6b and S6c). The result reveals that the $KMnO_4$/CNT system significantly decreases the bioaccumulation factor and acute toxicity of intermediates compared to the original SMX. For developmental toxicity, SMX is 0.85, some intermediates have lower toxicity than SMX (Fig. S6d). However, only one toxic intermediate is produced, especially the developmental toxicity of TP4 is 0.95. In all, the above results show that the CNT/$KMnO_4$ system cannot only accomplish the oxidation of SMX but also decreases the toxicity of SMX.

3.4 Stability evaluation of the $KMnO_4$/CNT system

Heterogeneous oxidation processes usually require robust catalysts for the practical applications. To demonstrate the exceptional stability of the $KMnO_4$/CNT system, the SMX degradation experiments were performed under optimal conditions for six continuous running cycles (Fig. 6(a)). As displayed in Fig. 6(b), there was almost no decrease in the SMX oxidation flux, and the mean oxidation flux was 2.42 mmol/(h·m^2), indicating a good stability of the proposed system. This is mainly attributed to the outstanding capacity of catalytic and electronic transfer of CNT. Besides, XRD patterns of the raw and used CNT in the $KMnO_4$/CNT system are presented in Fig. S7. The characteristic peaks of raw CNT were detected at 2θ = 25.80°, 40.08° and 53.03°, which can be indexed to the (110), (112), and (220) planes of crystal-

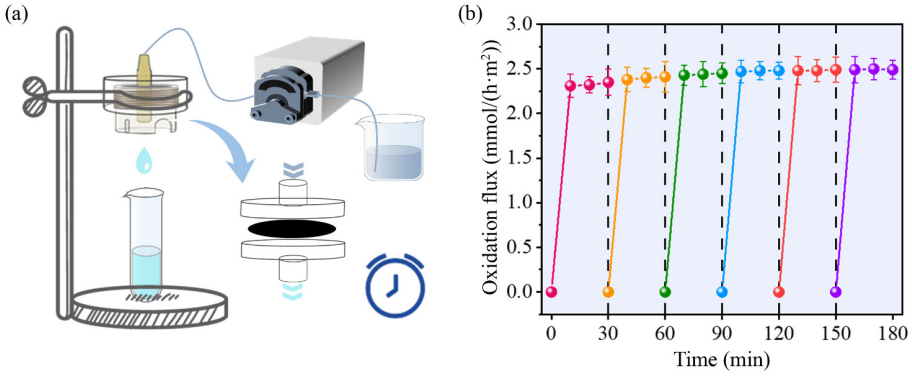

Fig. 6 (a) The schematic illustration of the $KMnO_4$/CNT system, and (b) the stability analysis for SMX oxidation flux. Experimental conditions: $[SMX]_0$ = 80 μmol/L, $[KMnO_4]_0$ = 1.0 mmol/L, flow rate = 0.5 mL/min, and pH = 6.2.

line CNT (JCPDS 89-8489). Meanwhile, no additional peaks were detected in the used CNT, indicating that CNT maintained a high level of stability after the reaction.

The speciation of $KMnO_4$ was closely correlated with the solution pH. Thus, the pH effect on the efficacy of the $KMnO_4$/CNT system was examined. As shown in Fig. S8, the SMX oxidation kinetics under acidic pH conditions was much higher than that of alkaline conditions. The oxidation flux of SMX decreased from 2.90 to 1.00 mmol/(h·m^2) in the $KMnO_4$/CNT system as the solution pH increased from 2.8 to 9.4. Moreover, the presence of CNT evidently contributed to the SMX oxidation as well, as evidenced by the elevated SMX removal in the $KMnO_4$/CNT system, as compared with that of $KMnO_4$ alone system. Hence, the acidic conditions are more favorable for the SMX oxidation in the $KMnO_4$/CNT system.

Wastewater is consisted of various coexisting ions, which deteriorates the efficiency of OCs degradation. Therefore, this study investigated whether common inorganic anions can affect the efficacy of the $KMnO_4$/CNT system. As displayed in Fig. S9, the $KMnO_4$/CNT system exhibited little impact on SMX oxidation after the addition of various inorganic anions (Cl^-, SO_4^{2-}, and NO_3^-), indicating its strong resistance to environmental interference.

Humic acid (HA), a typical and natural organic matter (NOM) in real waters, was selected to assess the effect of NOM on the $KMnO_4$/CNT system. HA has been shown to exert a positive effect the oxidation of OCs in the $KMnO_4$ system (Jiang et al., 2010; Sun et al., 2013; Xu et al., 2017; Gao et al., 2018). Interestingly, HA with low concentrations have little effect on SMX oxidation (Fig. S9). However, HA with a background concentration of 5.0 mg/L can inhibit SMX degradation, owing to the direct reaction of HA with $KMnO_4$. It has been reported that HA exhibits a reducing capacity, as it consists of reductive functional groups. As an electron donor that competes for $KMnO_4$ with SMX, HA can inhibit electron transfer from SMX to $KMnO_4$ (Peng et al., 2021).

To further verify the applicability of the $KMnO_4$/CNT system for OCs removal, the degradation of different refractory micropollutants that have wide pharmaceutical and industrial applications. As displayed in Fig. S10, benzoic acid and p-nitrophenol (electron-deficient contaminants) were difficult to undergo the electron-transfer reaction; while bisphenol A and SMX (electron-donating contaminants) were easy to undergo electron transfer reaction. These results indicated that the $KMnO_4$/CNT system could selectively and efficiently remove OCs with electron-donating. Taken together, our results demonstrate a novel flow-through system that enables robust, energy-effective, and high-efficiency water decontamination.

4 Conclusions

In this study, a flow-through $KMnO_4$/CNT system was designed for rapid and selective oxidization of OCs by enhancing the oxidation capacity of $KMnO_4$. The system demonstrated high performance and stability with efficient $KMnO_4$ utilization in environmental remediation. Extensive experimental studies and theoretical calculations revealed the electron-transfer mechanisms of the $KMnO_4$-based technologies. The excellent efficacy of the system was maintained in the presence of common anions, NOM, and an array of refractory micropollutants. The results of toxicity evaluation showed that the intermediates from SMX degradation had reduced toxicity. Hence, the $KMnO_4$/CNT system can serve as an efficient, cost-effective and sustainable advanced technology toward the remediation of OCs from water.

Acknowledgements This work was financially supported by the Natural Science Foundation of Shanghai (No. 23ZR1401300) and the National Natural Science Foundation of China (No. 52170068).

Electronic Supplementary Material Supplementary material is available in the online version of this article at https://doi.org/10.1007/s11783-023-1706-0 and is accessible for authorized users.

References

Bavasso I, Montanaro D, Di Palma L, Petrucci E (2020). Electrochemically assisted decomposition of ozone for degradation and mineralization of Diuron. Electrochimica Acta, 331: 135423

Casida M E, Jamorski C, Casida K C, Salahub D R (1998). Molecular excitation energies to high-lying bound states from time-dependent density-functional response theory: characterization and correction of the time-dependent local density approximation ionization threshold. Journal of Chemical Physics, 108(11): 4439–4449

Chen J, Qu R, Pan X, Wang Z (2016). Oxidative degradation of triclosan by potassium permanganate: kinetics, degradation products, reaction mechanism, and toxicity evaluation. Water Research, 103: 215–223

Chen J, Rao D, Dong H, Sun B, Shao B, Cao G, Guan X (2020). The role of active manganese species and free radicals in permanganate/bisulfite process. Journal of Hazardous Materials, 388: 121735

Cheng H, Ma J, Jiang J, Pang S Y, Yang T, Wang P (2019). Aggregation kinetics of manganese oxides formed from permanganate activated by (Bi)sulfite: dual role of Ca^{2+} and $Mn^{II/III}$. Water Research, 159: 454–463

Derakhshani E, Naghizadeh A (2013). Ultrasound regeneration of multi wall carbon nanotubes saturated by humic acid. Desalination and Water Treatment, 52(40–42): 7468–7472

Du J K, Xiao G F, Xi Y X, Zhu X W, Su F, Kim S H (2020). Periodate activation with manganese oxides for sulfanilamide degradation. Water Research, 169: 115278

Gao J, Hedman C, Liu C, Guo T, Pedersen J A (2012). Transformation of sulfamethazine by manganese oxide in aqueous solution.

Environmental Science & Technology, 46(5): 2642–2651

Gao Y, Jiang J, Zhou Y, Pang S Y, Ma J, Jiang C, Yang Y, Huang Z S, Gu J, Guo Q, Duan J B, Li J (2018). Chlorination of bisphenol S: kinetics, products, and effect of humic acid. Water Research, 131: 208–217

Gao Y, Zhou Y, Pang S Y, Jiang J, Yang Z, Shen Y, Wang Z, Wang P X, Wang L H (2019). New insights into the combination of permanganate and bisulfite as a novel advanced oxidation process: importance of high valent manganese-oxo species and sulfate radical. Environmental Science & Technology, 53(7): 3689–3696

Guan X H, He D, Ma J, Chen G H (2010). Application of permanganate in the oxidation of micropollutants: a mini review. Frontiers of Environmental Science & Engineering in China, 4(4): 405–413

Guo D L, You S J, Li F, Liu Y B (2022). Engineering carbon nanocatalysts towards efficient degradation of emerging organic contaminants *via* persulfate activation: a review. Chinese Chemical Letters, 33(1): 1–10

Han C, Duan X G, Zhang M J, Fu W Z, Duan X Z, Ma W J, Liu S M, Wang S B, Zhou X G (2019). Role of electronic properties in partition of radical and nonradical processes of carbocatalysis toward peroxymonosulfate activation. Carbon, 153: 73–80

Hao X M, Wang G L, Chen S, Yu H T, Quan X (2019). Enhanced activation of peroxymonosulfate by CNT-TiO_2 under UV-light assistance for efficient degradation of organic pollutants. Frontiers of Environmental Science & Engineering, 13(5): 77

Hu Y B, Lo S L, Li Y F, Lee Y C, Chen M J, Lin J C (2018). Autocatalytic degradation of perfluorooctanoic acid in a permanganate-ultrasonic system. Water Research, 140: 148–157

Jiang J, Pang S Y, Ma J (2010). Role of ligands in permanganate oxidation of organics. Environmental Science & Technology, 44(11): 4270–4275

Jin L, You S, Duan X, Yao Y, Yang J, Liu Y (2022). Peroxymonosulfate activation by Fe_3O_4-MnO_2/CNT nanohybrid electroactive filter towards ultrafast micropollutants decontamination: performance and mechanism. Journal of Hazardous Materials, 423: 127111

Kostka J E, Lutheriii G W, Nealson K H (1995). Chemical and biological reduction of Mn(III)-pyrophosphate complexes: potential importance of dissolved Mn(III) as an environmental oxidant. Geochimica et Cosmochimica Acta, 59: 885–894

Lee H, Kim H I, Weon S, Choi W, Hwang Y S, Seo J, Lee C, Kim J H (2016). Activation of persulfates by graphitized nanodiamonds for removal of organic compounds. Environmental Science & Technology, 50(18): 10134–10142

Liu Q Q, Li M, Liu X, Zhang Q, Liu R, Wang Z L, Shi X T, Quan J, Shen X H, Zhang F W (2018). Removal of sulfamethoxazole and trimethoprim from reclaimed water and the biodegradation mechanism. Frontiers of Environmental Science & Engineering, 12(6): 6

Liu Y B, Gao G D, Vecitis C D (2020). Prospects of an electroactive carbon nanotube membrane toward environmental applications. Accounts of Chemical Research, 53(12): 2892–2902

Liu Y B, Li J H, Zhou B X, Bai J, Zheng Q, Zhang J L, Cai W M (2009). Comparison of photoelectrochemical properties of TiO_2-nanotube-array photoanode prepared by anodization in different electrolyte. Environmental Chemistry Letters, 7(4): 363–368

Ma X Y, Hu S F, Wang H Y, Li J, Huang J, Zhang Y, Lu W G, Li Q S (2012). Kinetics of oxidation of dimethyl trisulfide by potassium permanganate in drinking water. Frontiers of Environmental Science & Engineering, 6(2): 171–176

Mustafa M, Wang H J, Lindberg R H, Fick J, Wang Y Y, Tysklind M (2021). Identification of resistant pharmaceuticals in ozonation using QSAR modeling and their fate in electro-peroxone process. Frontiers of Environmental Science & Engineering, 15(5): 106

Pan F, Ji H, Du P, Huang T, Wang C, Liu W (2021). Insights into catalytic activation of peroxymonosulfate for carbamazepine degradation by MnO_2 nanoparticles in-situ anchored titanate nanotubes: mechanism, ecotoxicity and DFT study. Journal of Hazardous Materials, 402: 123779

Pearson R G (1986). Absolute electronegativity and hardness correlated with molecular orbital theory. Proceedings of the National Academy of Sciences of the United States of America, 83(22): 8440–8441

Peng J, Zhou P, Zhou H, Liu W, Zhang H, Zhou C, Lai L, Ao Z, Su S, Lai B (2021). Insights into the electron-transfer mechanism of permanganate activation by graphite for enhanced oxidation of sulfamethoxazole. Environmental Science & Technology, 55(13): 9189–9198

Rasool K, Pandey R P, Rasheed P A, Buczek S, Gogotsi Y, Mahmoud K A (2019). Water treatment and environmental remediation applications of two-dimensional metal carbides (MXenes). Materials Today, 30: 80–102

Ren W, Xiong L L, Nie G, Zhang H, Duan X G, Wang S B (2020). Insights into the electron-transfer regime of peroxydisulfate activation on carbon nanotubes: the role of oxygen functional groups. Environmental Science & Technology, 54(2): 1267–1275

Shao P, Yu S, Duan X, Yang L, Shi H, Ding L, Tian J, Yang L, Luo X, Wang S (2020). Potential difference driving electron transfer *via* defective carbon nanotubes toward selective oxidation of organic micropollutants. Environmental Science & Technology, 54(13): 8464–8472

Shen Z C, Zhan L, Xu Z M (2022). Thermal defluorination behaviors of PFOS, PFOA and PFBS during regeneration of activated carbon by molten salt. Frontiers of Environmental Science & Engineering, 16(8): 103

Shi Z, Jin C, Bai R, Gao Z, Zhang J, Zhu L, Zhao Z, Strathmann T J (2020). Enhanced transformation of emerging contaminants by permanganate in the presence of redox mediators. Environmental Science & Technology, 54(3): 1909–1919

Simandi L I, Jaky M, Schelly Z A (1984). Short-lived manganate(VI) and manganate(V) intermediates in the permanganate oxidation of sulfite ion. Journal of the American Chemical Society, 106(22): 6866–6867

Sun B, Guan X H, Fang J Y, Tratnyek P G (2015). Activation of manganese oxidants with bisulfite for enhanced oxidation of organic contaminants: the Involvement of Mn(III). Environmental Science & Technology, 49(20): 12414–12421

Sun B, Xiao Z, Dong H, Ma S, Wei G, Cao T, Guan X (2019). Bisulfite triggers fast oxidation of organic pollutants by colloidal MnO_2. Journal of Hazardous Materials, 363: 412–420

Sun B, Zhang J, Du J S, Qiao J L, Guan X H (2013). Reinvestigation of

the role of humic acid in the oxidation of phenols by permanganate. Environmental Science & Technology, 47(24): 14332–14340

Tang L, Liu Y, Wang J, Zeng G, Deng Y, Dong H, Feng H, Wang J, Peng B (2018). Enhanced activation process of persulfate by mesoporous carbon for degradation of aqueous organic pollutants: electron transfer mechanism. Applied Catalysis B: Environmental, 231: 1–10

Tian S Q, Wang L, Liu Y L, Yang T, Huang Z S, Wang X S, He H Y, Jiang J, Ma J (2019). Enhanced permanganate oxidation of sulfamethoxazole and removal of dissolved organics with biochar: formation of highly oxidative manganese intermediate species and in situ activation of biochar. Environmental Science & Technology, 53(9): 5282–5291

Wang X, Wang Y, Zhao C, Zhu Y, Sun Z, Fan H S, Hu X, Zheng H (2021). Ciprofloxacin removal by ultrasound-enhanced carbon nanotubes/permanganate process: *in situ* generation of free reactive manganese species *via* electron transfer. Water Research, 202: 117393

Wu L, Wu T, Liu Z, Tang W, Xiao S, Shao B, Liang Q, He Q, Pan Y, Zhao C, Liu Y, Tong S (2022). Carbon nanotube-based materials for persulfate activation to degrade organic contaminants: properties, mechanisms and modification insights. Journal of Hazardous Materials, 431: 128536

Xu K, Ben W, Ling W, Zhang Y, Qu J, Qiang Z (2017). Impact of humic acid on the degradation of levofloxacin by aqueous permanganate: kinetics and mechanism. Water Research, 123: 67–74

Yang S, Wang S, Liu X, Li L (2019). Biomass derived interconnected hierarchical micro-meso-macro-porous carbon with ultrahigh capacitance for supercapacitors. Carbon, 147: 540–549

Yu S, Peng Y, Shao P, Wang Y, He Y, Ren W, Yang L, Shi H, Luo X (2023). Electron-transfer-based peroxymonosulfate activation on defect-rich carbon nanotubes: understanding the substituent effect on the selective oxidation of phenols. Journal of Hazardous Materials, 442: 130108

Yun E T, Lee J H, Kim J, Park H D, Lee J (2018). Identifying the nonradical mechanism in the peroxymonosulfate activation process: singlet oxygenation versus mediated electron transfer. Environmental Science & Technology, 52(12): 7032–7042

Zhang P, Zhou P, Peng J L, Liu Y, Zhang H, He C S, Xiong Z K, Liu W, Lai B (2022). Insight into metal-free carbon catalysis in enhanced permanganate oxidation: changeover from electron donor to electron mediator. Water Research, 219: 118626

Zheng W T, You S J, Yao Y, Jin L M, Liu Y B (2021). Development of atomic hydrogen-mediated electrocatalytic filtration system for peroxymonosulfate activation towards ultrafast degradation of emerging organic contaminants. Applied Catalysis B: Environmental, 298: 120593

Zhou Y, Gao Y, Jiang J, Shen Y M, Pang S Y, Song Y, Guo Q (2021). A comparison study of levofloxacin degradation by peroxymonosulfate and permanganate: kinetics, products and effect of quinone group. Journal of Hazardous Materials, 403: 123834

Zhou Z, Liu X, Sun K, Lin C Y, Ma J, He M C, Ouyang W (2019). Persulfate-based advanced oxidation processes (AOPs) for organic-contaminated soil remediation: a review. Chemical Engineering Journal, 372: 836–851

Zhu S S, Huang X C, Ma F, Wang L, Duan X G, Wang S B (2018). Catalytic removal of aqueous contaminants on N-doped graphitic biochars: inherent roles of adsorption and nonradical mechanisms. Environmental Science & Technology, 52(15): 8649–8658

Zhu Y H, Wang X X, Zhang J, Ding L, Li J F, Zheng H L, Zhao C (2019a). Generation of active $Mn(III)_{aq}$ by a novel heterogeneous electro-permanganate process with manganese(II) as promoter and stabilizer. Environmental Science & Technology, 53(15): 9063–9072

Zhu Y H, Zhao C, Liang J L, Shang R, Zhu X M, Ding L, Deng H P, Zheng H L, Strathmann T J (2019b). Rapid removal of diclofenac in aqueous solution by soluble $Mn(III)_{aq}$ generated in a novel electro-activated carbon fiber-permanganate (E-ACF-PM) process. Water Research, 165: 114975